Magnetic Resonance Materials in Physics, Biology and Medicine
https://doi.org/10.1007/s10334-020-00883-z

RESEARCH ARTICLE

Contrast optimization in arterial spin labeling with multiple post-labeling delays for cerebrovascular assessment

André Monteiro Paschoal[1,3] · Renata Ferranti Leoni[1] · Bernd Uwe Foerster[2] · Antonio Carlos dos Santos[3] · Octávio Marques Pontes-Neto[3] · Fernando Fernandes Paiva[2]

Received: 2 April 2020 / Revised: 1 July 2020 / Accepted: 25 August 2020

Abstract

Objective Improving the readout for arterial spin labeling with multiple post-labeling delays (multi-PLD ASL) through a flip angle (FA) sweep towards increasing contrast-to-noise ratio for long PLD images.

Methods Images were acquired from 20 healthy subjects and 14 patients with severe, asymptomatic carotid artery stenosis (ACAS) in a 3T MRI scanner. Multi-PLD ASL images with conventional and proposed (FA sweep) readouts were acquired. For patients, magnetic resonance angiography was used to validate the multi-PLD ASL results. Perfusion values were calculated for brain regions irrigated by the main cerebral arteries and compared by analysis of variance.

Results For healthy subjects, better contrast was obtained for long PLDs when using the proposed multi-PLD method compared to the conventional. For both methods, no hemispheric difference of perfusion was observed. For patients, the proposed method facilitated the observation of delayed tissue perfusion, which was not visible for long PLD using the conventional multi-PLD ASL.

Conclusion We successfully assessed brain perfusion of patients with asymptomatic CAS using multi-PLD ASL with FA sweep. We were able to show subtle individual differences. Moreover, prolonged arterial transit time in patients was observed, although they were considered asymptomatic, suggesting that it may not be an adequate term to characterize them.

Keywords Arterial spin labeling · Flip angle sweep · Multiphase · Brain · Perfusion

Introduction

Cerebral Blood Flow (CBF) is an important parameter for the investigation of brain hemodynamics, since a variation of blood flow in brain arteries might severely affect tissue perfusion and neurological functions. It is particularly true in neurovascular disorders, such as stroke [1, 2], which is strongly associated with the carotid artery stenosis (CAS) or occlusion due to arterial embolism and hemodynamic compromise [1]. Patients with CAS may be asymptomatic, i.e., with no incidence of ipsilateral stroke and transient ischemic attack (TIA), but present cognitive decline [3]. Moreover, the patient selection for intervention in these cases is still controversial. Therefore, the ability to properly assess CBF with noninvasive methods is a major determinant for our understanding of the relation between atherosclerotic disease, altered perfusion, and neurological impairment in asymptomatic CAS (ACAS).

Arterial Spin Labeling (ASL) is a noninvasive, perfusion-based magnetic resonance imaging (MRI) method that quantifies CBF in units of mL/min/100 g of tissue [4, 5] and enables prolonged monitoring of cerebral perfusion. The measurement of brain perfusion with ASL requires the acquisition of a labeled image, where arterial blood is tagged with a radiofrequency (RF) pulse, and a control image, where no preparation pulse is used before its acquisition. Therefore, CBF

Electronic supplementary material The online version of this article (https://doi.org/10.1007/s10334-020-00883-z) contains supplementary material, which is available to authorized users.

✉ Fernando Fernandes Paiva
fernando.paiva@usp.br

[1] Inbrain, Faculdade de Filosofia, Ciências e Letras de Ribeirão Preto, Universidade de São Paulo, Ribeirão Preto, SP, Brazil

[2] Instituto de Física de São Carlos, Universidade de São Paulo, Av. Trabalhador São-Carlense, 400, São Carlos, SP 13566-590, Brazil

[3] Faculdade de Medicina de Ribeirão Preto, Universidade de São Paulo, Ribeirão Preto, SP, Brazil

Published online: 03 September 2020

is proportional to the difference between control and label images. An accurate estimation of CBF relies on the acquisition of images at an appropriate time after spins have been tagged, and tagged blood must reach the image plane before data acquisition. The interval between labeling and acquisition is called post-labeling delay (PLD), and its optimization depends on the arterial blood transit time (ATT). Since patients with ACAS may present delayed ATT, an accurate CBF assessment requires an acquisition independent of the PLD choice [6, 7]. The elimination of such dependency is possible with acquisitions at different PLDs. In such a case, each acquisition is a phase, and the method is called multiphase ASL or multi-PLD ASL.

Multi-PLD ASL has been used for different applications, such as measurement of arterial transit time (ATT) [8–10], characterization of cerebral border zones [11], and assessment of water extraction across the blood–brain barrier [11–14]. Different acquisition approaches have been developed to improve the signal-to-noise ratio (SNR) and acquisition time efficiency through the use of Look-Locker readout [15–19] and time-encoded schemes, as the Hadamard [16, 20, 21]. However, the image contrast at later delays is hampered by a repeated application of excitation pulses and longitudinal relaxation, which affect the evaluation of tissue perfusion in regions where the transit time is longer. Therefore, we propose a readout flip angle modulation to the Look–Locker approach for the acquisition of images with good contrast-to-noise ratio (CNR), even for long PLDs, towards overcoming the limitation of conventional Look–Locker methods with a fixed readout flip angle for all the PLDs. We used the method to evaluate cerebral perfusion healthy volunteers and in patients with ACAS. We hypothesize that such patients present delayed ATT and brain hypoperfusion related to the stenosis and that our approach may offer an efficient, but simple tool for such evaluation.

Materials and methods

Flip angle modulation

A multi-PLD ASL acquisition with flip angle α, m phases, an interval τ between two consecutive phases, and longitudinal relaxation time T_1 of the blood was assumed for the calculation of the modulation equation, given by Eq. 1:

$$\Delta M_m = 2M_0 e^{-\left[\frac{T_1+(m-1)\tau}{T_1}\right]} \sin\left(\alpha_m\right) \times \begin{cases} 1, & \text{if } m = 1 \\ \prod_{i=1}^{m-1} \cos\left(\alpha_m\right), & \text{if } m > 1 \end{cases}. \tag{1}$$

The proposed approach calculates the flip angles to keep the magnetization difference constant over the phases. In a general way, the flip angle for the *ith* phase for a total of m phases is given by:

$$\alpha_i = \tan^{-1}\left(\frac{\sin\left(\alpha_m\right)\exp\left(-\frac{(m-i)\tau}{T_1}\right)}{\sqrt{1+\sum_{k=1}^{m-i-1}\sin^2\left(\alpha_m\right)\exp\left(-\frac{2k\tau}{T_1}\right)}} \right), i = 1 \ldots (m-1), \tag{2}$$

where α_m must be defined by the user according to the repetition and relaxation times (detailed description for the FA sweep equation is in supplementary material). The flip angle shown in Eq. 2 is then applied to both control and label images, so that the static tissue will be the same for both conditions. Therefore, after the control-label subtraction, static tissue magnetization will greatly reduce, resulting only in a perfusion signal.

Subjects

Fourteen patients (5 females; mean age ± standard deviation (SD) = 72 ± 7, range 56–83) and twenty healthy volunteers (8 females; mean age ± SD = 26 ± 9, range 18–47) participated in this cross-sectional study, approved by the Institutional Review Board, after signing informed consent. Patients were recruited at the Clinical Hospital of the institution, and the inclusion criterion was severe (≥ 70%), unilateral CAS, or occlusion, identified by an experienced neuroradiologist using the patient's MR angiography (MRA). The sample size was determined by the number of patients who met the criteria and agreed to participate during the study period (1 year). For all subjects, the exclusion criteria were a history of any cerebrovascular event (stroke, transient ischemic attack); the presence of neurologic disorders, such as epilepsy, multiple sclerosis, amyotrophic lateral sclerosis, brain tumor, and dementia; psychiatric disorders; pregnancy; claustrophobia; contraindications for MRI. The healthy volunteers were recruited to compose a dataset for the evaluation of the quality of the images acquired with the proposed method.

MR system

Data were collected at a 3T MR system (Achieva, Philips Medical Systems, Holland), equipped with gradients of 80 mT/m amplitude and 200 mT/m/ms slew rate. We used a standard transmit body coil and a 32-channel receive-only head coil.

Scanning protocols

The MRI protocol consisted of a whole-brain structural image acquired by a three-dimensional T1-weighted (3DT1) GRE-EPI sequence with 240 × 240 mm^2 field-of-view

(FOV), 164 1-mm-thick slices and TR/TE = 6.2/2.8 ms. A conventional PULSAR (pulsed STAR labeling of arterial regions) sequence [19] was modified for the use of variable flip angles during the acquisition of the multiple ASL phases. In the same MRI session, two multi-PLD ASL sequences (with and without flip angle modulation) were acquired with the following parameters: TR/TE = 4000/18 ms, FOV = 240 × 240 mm^2, in-plane resolution = 3.75 mm × 3.75 mm (acquisition matrix = 64 × 64), number of slices = 6, slice thickness = 6 mm, number of phases = 8, and number of repetitions = 35. PLDs varied between 900 and 2825 ms, with a time interval (τ) of 275 ms between each consecutive phase. For the FA sweep method, the flip angle for all the PLDs were 11.01º, 12.96º, 15.38º, 18.49º, 22.65º, 28.74º, 39.19º, and 70º, obtained from Eq. 2. For the conventional method, a flip angle of 30º was used for all PLDs. A 200-mm-wide tagging region was positioned 10 mm below the imaging region. Two time-of-flight (TOF) angiograms were acquired for the visualization of the Internal Carotid Arteries (ICAs) and Vertebral Arteries (VAs).

Data processing

Data were processed using SPM (version 12, Wellcome Trust Center for Neuroimaging, University College London, UK) and custom scripts in Matlab (Mathworks, MA, USA). Raw label and control images were realigned, resliced, and co-registered to anatomical images. Maps of magnetization difference (ΔM) were calculated by subtracting labeled and control images.

ATT maps were estimated by finding the maximum of ASL signal intensity throughout the multiple post-labeling delays. Prior to that, the time interval between the first and the last PLD was linear spaced in 1000 time points, and the linear interpolation of ASL signal value was estimated for every point.

CBF quantification based on the kinetic model [22] was performed using the BASIL toolkit of the Oxford Centre for Functional MRI of the BRAIN (FMRIB)'s software library (FSL) [23, 24], after correcting the ASL signal for Look–Locker effects dividing the ASL images by the sine of FA [18]. Gray matter (GM) and white matter (WM) masks were obtained after running FSL FLIRT [25] to corregister T1-weighted images to the ASL low-resolution space and FSL FAST [25] to segment into the partial volume for GM, WM, and CSF.

Data analysis

The signal evolution of ΔM was analyzed in Regions of Interest (ROI) defined according to the arteries that feed the respective vascular territory, i.e., anterior cerebral artery (ACA), middle cerebral artery (MCA), and posterior cerebral artery (PCA), for both hemispheres. Mean perfusion values of each ROI were obtained. For healthy subjects, comparisons between regions and phases were made using analysis of variance. Statistical significance was considered for $p < 0.05$. It was also calculated the spatial signal-to-noise ratio (sSNR) of the GM (sSNR = mean GM signal/stand deviation GM signal) as well as the contrast-to-noise ratio (CNR) [CNR = (mean GM signal − mean WM signal)/(standard deviation GM signal + stand deviation WM signal)] to measure the gain of the proposed implementation.

Patients' images were independently reviewed and assessed by two specialists for diagnostic purposes. A neuroradiologist (A.C.S) with 34 year experience analyzed structural images and MRA. A neurologist (O.M.P.N) with 17 year experience in cerebrovascular diseases with no knowledge of previous reports of the patients analyzed the ASL maps (with and without FA sweep). Each patients' dataset was individually analyzed, since patients differed from each other regarding stenosis side and severity. The CNR for each patient was calculated by comparing the GM and WM signal in the ROI indicated by the neurologist. For both control and patients group, differences in sSNR and CNR for each phase were statistically assessed by the application of a paired t test using the Bonferroni criteria for correction for multiple comparisons, which considered $p < 0.00625$ for statistical significance.

Results

Method evaluation in healthy volunteers

Data from healthy volunteers were used for the assessment of the FA sweep method. Figure 1 shows perfusion maps from a representative volunteer. Three slices and all eight phases acquired by the proposed FA sweep (Fig. 1a) and the conventional fixed FA (Fig. 1b) are shown. For the initial phases, i.e., shorter PLDs, both methods provided perfusion maps with sufficient contrast for visual inspection. However, the loss of contrast became apparent throughout the later phases for the conventional implementation, which hampered the perfusion analysis for long PLDs. The flip angle modulation circumvented this problem and enabled a precise evaluation of perfusion for all phases acquired. While, for conventional implementation, the signal dropped after reaching its maximum, the use of flip angle sweep led to a sufficient contrast throughout the phases. Furthermore, ATT maps were directly estimated for the FA sweep method by taking the post-labeling delay that had the maximal ASL signal intensity, as exemplified for one healthy subject in Fig. 2.

Considering all regions, we observed differences in signal intensity between phases. For the FA sweep method,

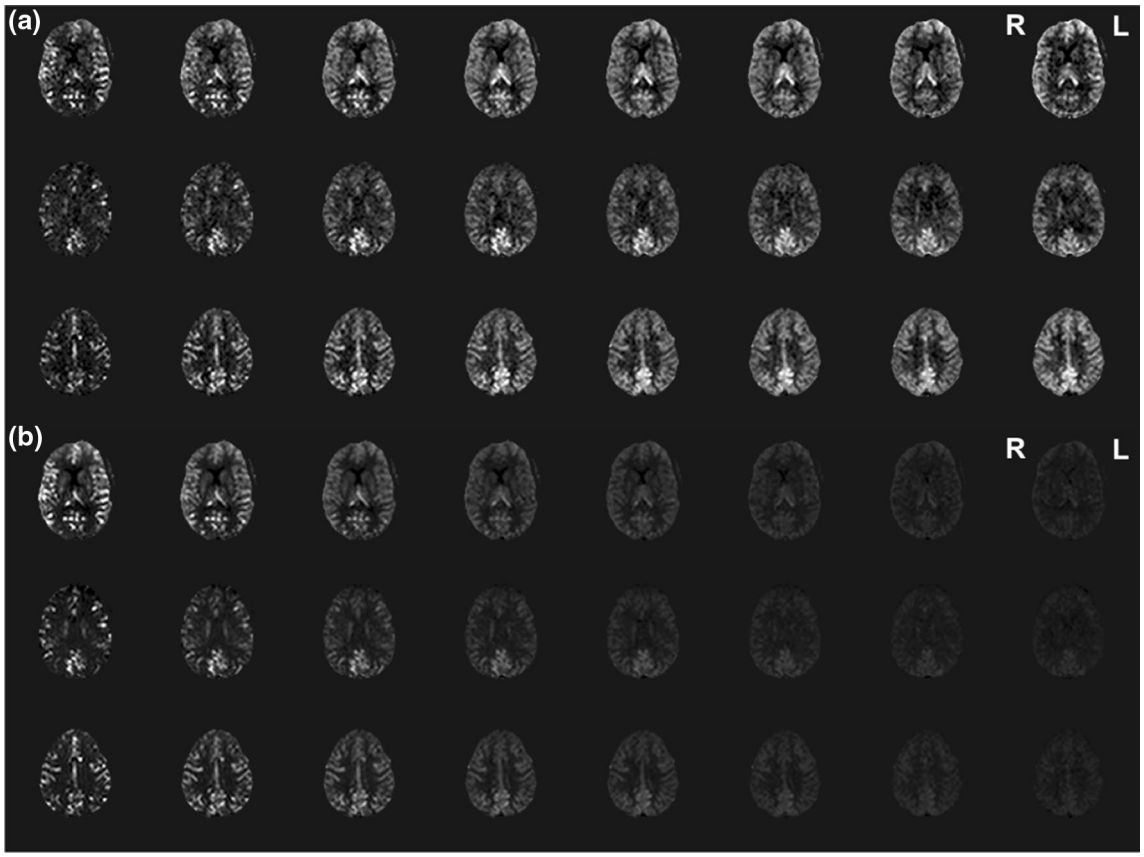

Fig. 1 Perfusion maps of a representative, healthy control. Three slices (rows) for all eight phases (columns) acquired by **a** the proposed multiphase method with flip angle sweep and **b** conventional multiphase arterial spin labeling method. R: right, L: left

signal intensity was significantly lower for phases 1 and 2 ($p < 0.05$). For the conventional map, signal intensity was significantly lower from phase 5 up to the last phase ($p < 0.05$), confirming the visual analysis. This pattern is also quantitatively described through the sSNR measurement, as shown in Fig. 3a, which resulted in increased values when using the FA sweep modulation ($p < 0.00625$ for all phases). Moreover, for both methods, no difference in signal intensity between hemispheres was observed ($p > 0.05$); however, the analysis of variance showed a significant effect of region on such values ($p < 0.05$). Higher values were observed in brain areas irrigated by the posterior circulation, typical of healthy young subjects. For the FA sweep method, this result was observed from phase 4 up to phase 8. However, for the conventional method, it was only observed for phases 4, 5, and 6. The CNR showed in Fig. 3b was significantly higher for the conventional method in the first 4 phases ($p < 0.00625$). For phases 7 and 8, it was significantly higher for the FA sweep method ($p < 0.00625$).

CBF maps were obtained for all healthy volunteers. The average gray matter CBF was 46 ± 11 mL/100 g/min for the FA sweep method and 39 ± 7 mL/100 g/min for the FA fixed method.

Patient analysis

The reports from two specialists are shown in Table 1. For each patient, both reports were considered to determine the performance of multi-PLD ASL with FA sweep in comparison with MRA findings. The overall comparison revealed an agreement of 85%. Additionally, for the conventional method, in 57% of the patients, the neurologist could not give a precise diagnosis, or the diagnosis was incorrect compared to the MRA. All correct diagnoses provided by the conventional method were also correct using the FA sweep approach.

Figure 4 shows data of a patient with an occlusion in the right ICA and a severe stenosis of 90% in the left ICA, as indicated in the TOF image (Fig. 4a, b, Table 1—P05). The analysis of the multi-PLD ASL maps with flip angle modulation (Fig. 4c) revealed an apparent reduction in CBF in the right MCA territory in the initial phases (red arrows). Tissue perfusion started first in the left hemisphere (phases 1, 2, and 3) with delayed transit time (Fig. 5a). For later phases, we observed collateral flow, i.e., blood from arteries in the left hemisphere irrigating regions of the right hemisphere, which resulted in CBF on the right side of the brain. With

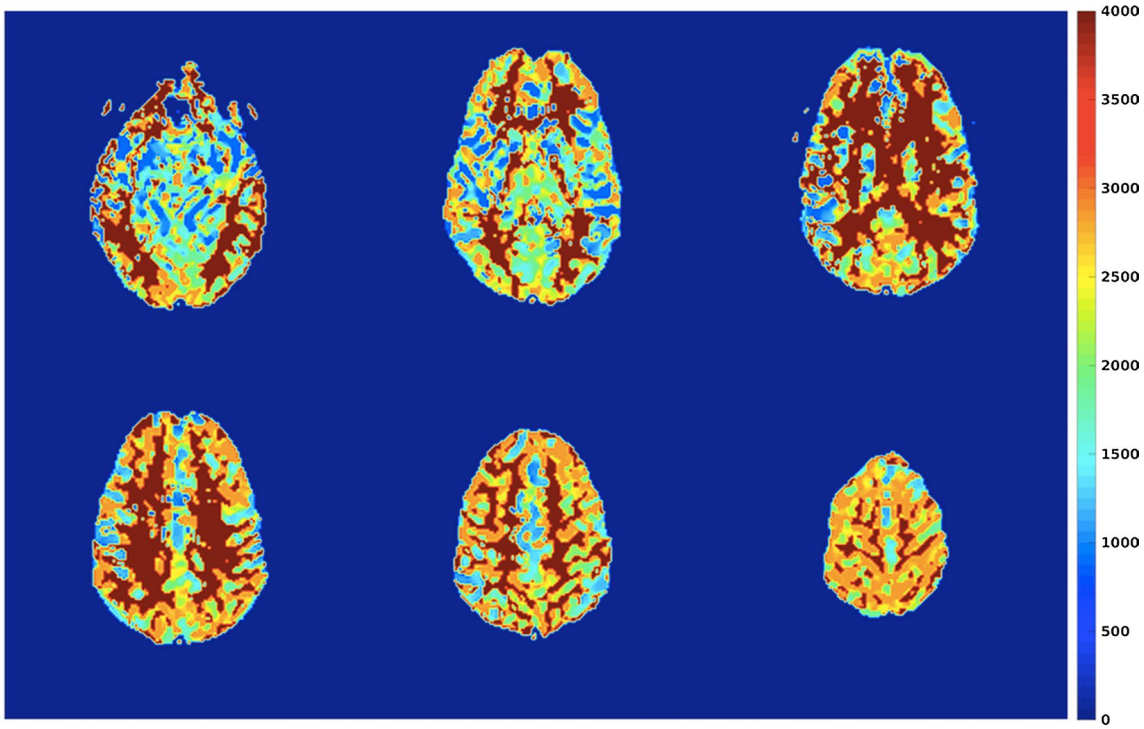

Fig. 2 Arterial transit time (ATT) map for a representative healthy subject. Color scale is in ms

the conventional multi-PLD ASL method (Fig. 4d), such analysis was impaired due to the loss of CNR for long PLDs.

Figure 6 shows the data of a patient with mild stenosis in the right ICA (Table 1—P07). The intracranial angiography revealed blood flow arriving in the intracranial arteries (Fig. 6a, b). Figure 6c displays ASL maps acquired by the FA sweep method, which showed a small increase in the arterial transit time on the right hemisphere (2.96 s for ipsi-PCA vs. 2.90 s for contra-PCA), which resulted in a slight reduction of blood perfusion at the right MCA territory in the first phases (red arrows). With the FA sweep method (Fig. 6c), it was possible to monitor blood perfusion over the phases, which revealed that it reached a similar value at both hemispheres for long PLDs.

Figure 7 shows data of a patient with severe stenosis of 70% in the left ICA (Table 1—P08), as indicated in the TOF image (Fig. 7a, b). The analysis of the multi-PLD ASL maps with flip angle modulation (Fig. 7c) revealed a slight reduction in CBF in the left MCA territory in initial phases (red arrows). Tissue perfusion has a reduction in the left hemisphere (phases 1, 2, and 3) with delayed transit time, whose average was 3.09 s for ipsi-MCA and 2.86 s for contra-MCA. For later phases, we observed more homogeneous brain perfusion. With the conventional multi-PLD ASL method (Fig. 7d), this behavior could not be seen due to the loss of CNR for long PLDs. CNR evolution for the MCA territory is shown in Fig. 8.

Figure 9 shows data of a patient with an obstruction in the left ICA and moderate (50%) stenosis in the right ICA (Table 1—P13) (Fig. 9a, b). The ASL maps (Fig. 9c) revealed an increase in the arterial transit time on both hemispheres, but more pronounced in the left hemisphere with delayed blood flow (Fig. 5d), especially in the first phases. The entire left hemisphere presented blood perfusion reduction due to reduced flow in the circle of Willis, as verified in the TOF image (Fig. 9b). For longer PLD, there was an increase in blood perfusion due to compensation mechanisms. Such analysis is compromised when data were acquired with the conventional approach (Fig. 9d).

The benefits visually observed in the analysis of the previous examples of patients are enhanced by the CNR measurement in the ROIs of delayed blood flow indicated by the neurologist. The bar plot in Fig. 10 represents the normalized mean CNR for all the 13 patients included in this study, revealing a significant increase in the CNR for the latter two phases ($p < 0.00625$).

The quantitative results of CBF measurements are shown in Fig. 11 for a representative healthy control and for all the exemplified patients. For comparison, CBF maps for both sweep and fixed FA are reported.

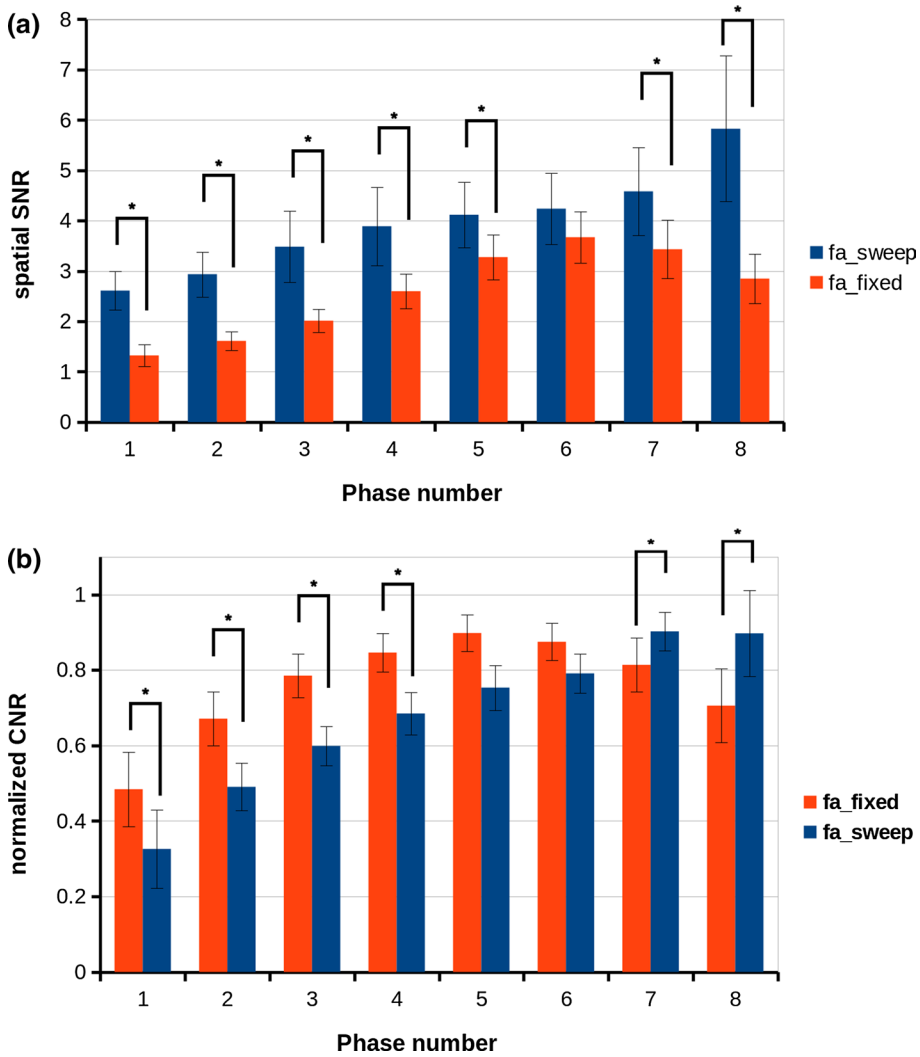

Fig. 3 Mean gray matter: **a** spatial signal-to-noise ratio and **b** normalized contrast-to-noise ration for all 20 healthy subjects (mean ± standard deviation) for the FA sweep (blue) and FA fixed (red) methods (*p-FWE < 0.00625)

Discussion

We proposed an approach for the multiphase ASL method to guarantee sufficient contrast for perfusion images acquired at long PLDs. First, images were acquired from healthy controls. Perfusion maps showed a better contrast for the proposed method compared to the conventional Look–Locker readout with fixed FA approach for long PLDs, and an increased sSNR for all the PLDs acquired and higher CNR for the last two PLDs. For both methods, no hemispheric difference of perfusion was observed; however, regions irrigated by the posterior cerebral artery showed higher perfusion values, as expected for healthy, young subjects [26]. Furthermore, the ATT map for a representative subject showed a result in agreement with the expected for healthy subjects [27, 28].

Moreover, we investigated the cerebral perfusion of patients with asymptomatic carotid artery stenosis. The visual comparison of images acquired by both methods revealed essential differences between them, mainly for later phases. The inspection of the perfusion maps obtained for different PLDs was not crucial for healthy controls, in which no alteration in blood transit times is expected, and gray matter is already perfused at first phases. However, patients with arterial stenosis or occlusion may present a delayed transit time. Therefore, the assessment of all phases was necessary for the analysis.

Recent studies have used ASL with at least two PLD values to obtain maps of arterial transit time and quantify CBF with better accuracy [8, 29, 30]. The previous studies have reported methods to improve the CNR of ASL images for long PLDs [31, 32]. Our approach used a maximum PLD of 2825 ms, longer than the ones previously reported [33, 34], and allowed the dynamic assessment of tissue perfusion, including the presence of collateral flow by significantly increasing the sSNR for all the PLDs and especially resulting in significant differences for the CNR of latter phases (Fig. 10). Moreover, it did not require any mathematical models to quantify the arterial transit time (Fig. 5), being more appealing for clinical use.

Table 1 Patients' information and specialists' reports

ID	Gender	Age	Report 1[a]	Report 2[b]
P01	Female	56	Critical stenosis on the ICA with flow reduction on the right MCA territory	Flow reduction on the right MCA vascular territory
P02	Female	68	Critical stenosis on the right side of carotid bulb with flow reduction on the right MCA	Flow reduction on the right MCA vascular territory
P03	Male	77	Critical stenosis on the left ICA with flow reduction in the territory of posterior communicant arteries	Flow reduction on the left PCA vascular territory
P04	Male	83	Critical stenosis on the left ICA	Flow reduction on the left MCA vascular territory
P05	Male	77	Occlusion of the right ICA and critical stenosis on left ICA with severe flow reduction in right MCA territory	Flow reduction on the right MCA vascular territory
P06	Female	81	Critical stenosis on the left ICA without a change in flow	No flow reduction
P07	Male	70	Discreet stenosis on the right ICA and severe stenosis on the left external carotid artery	Slight flow reduction on the right MCA vascular territory and left PCA vascular territory
P08	Female	65	Critical stenosis on the left ICA with a slight change in flow	Slight flow reduction on the left MCA vascular territory
P09	Male	70	Critical stenosis on the right ICA with small flow reduction on the right hemisphere	Flow reduction on the right MCA vascular territory
P10	Male	67	Critical stenosis on the right ICA	Flow reduction on the right MCA and left PCA vascular territories
P11	Male	77	Excluded due to motion	Excluded due to motion
P12	Male	67	Occlusion of the left ICA and moderate stenosis on the right ICA	Flow reduction on the left hemisphere
P13	Female	70	Critical stenosis on right ICA with flow reduction at the right side of the circle of Willis	Flow reduction on the right MCA vascular territory
P14	Male	65	Critical stenosis on the right ICA and discreet stenosis on the left ICA	No significant change in flow

ICA internal carotid artery, *MCA* middle carotid artery, *PCA* posterior carotid artery

[a]From MR angiography and Doppler ultrasound

[b]From multiphase ASL with flip angle sweep

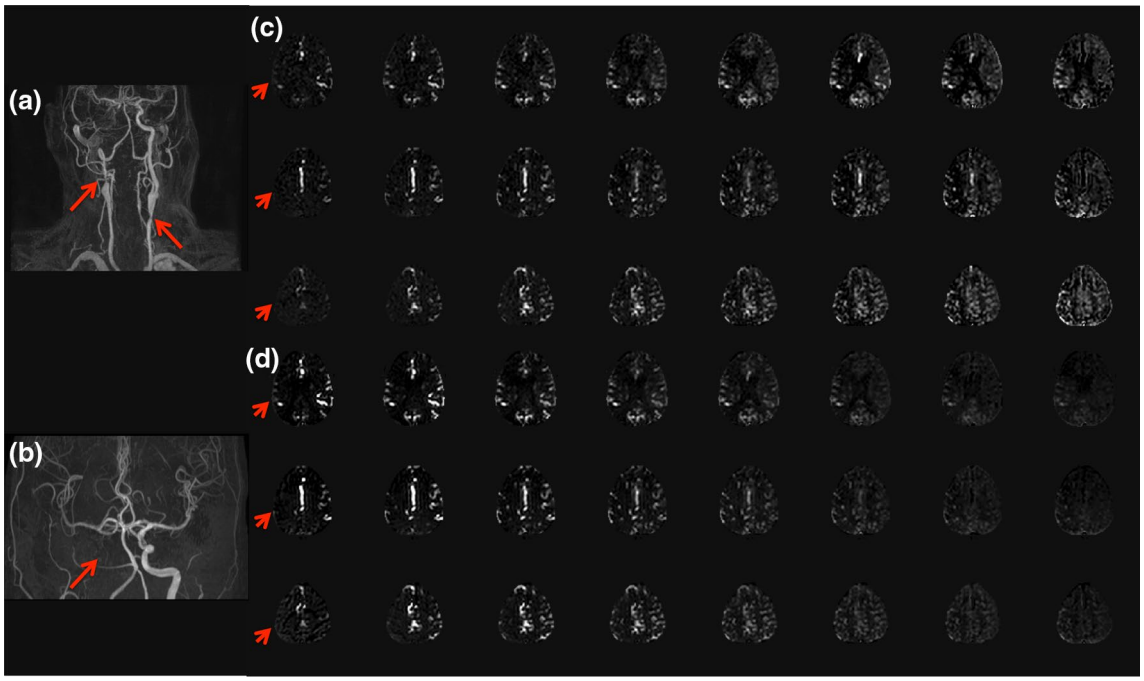

Fig. 4 Data from a patient with an occlusion in the right ICA and a 90% severe stenosis in the left ICA. **a** Carotid and **b** intracranial angiography. Multiphase maps **c** with and **d** without flip angle sweep

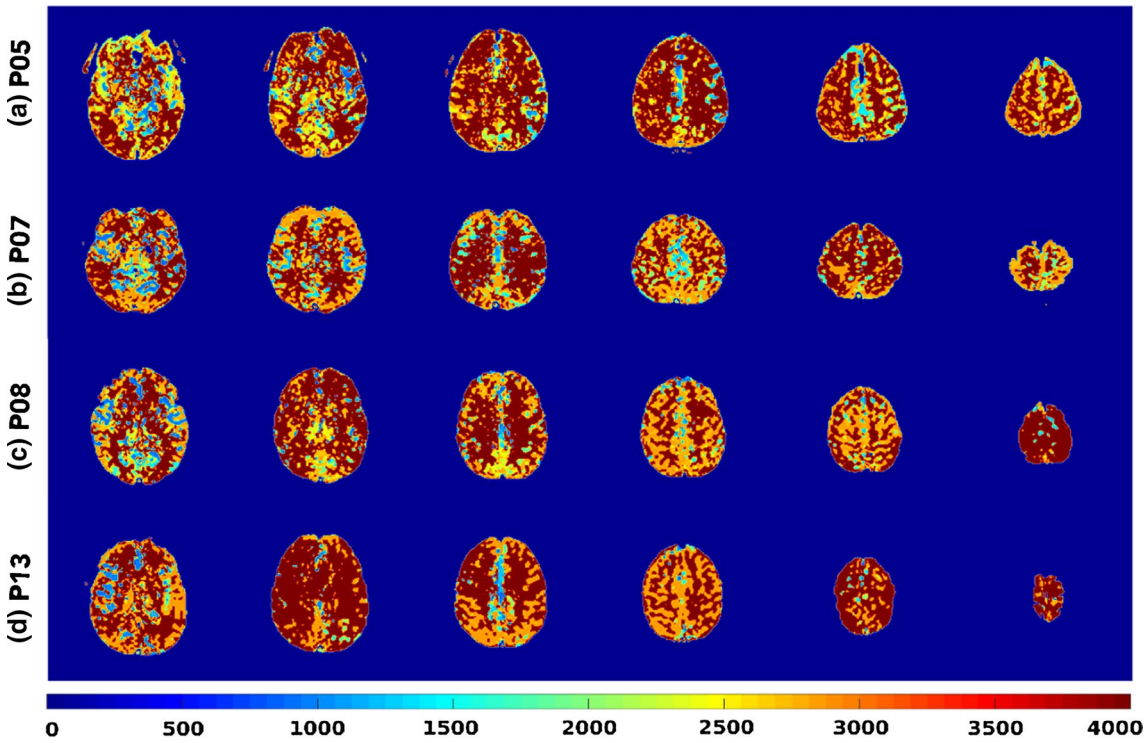

Fig. 5 Arterial transit time (ATT) maps for four patients. Color scale is in ms

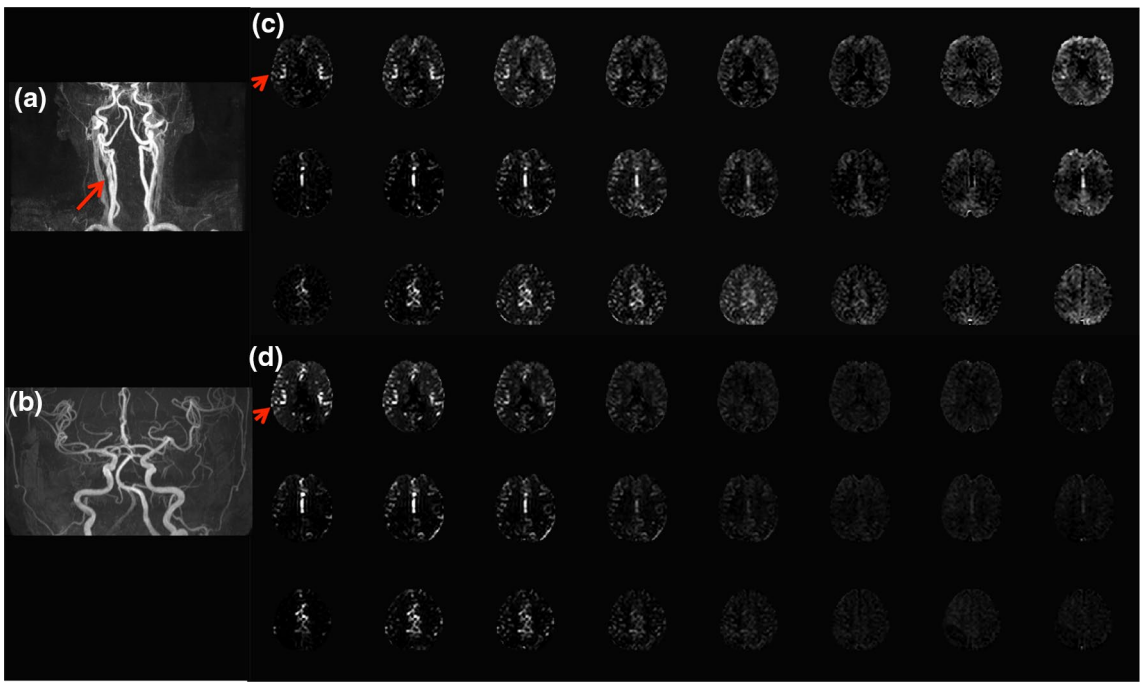

Fig. 6 Data from a patient with mild stenosis in the right ICA. **a** Carotid and **b** intracranial angiography. Multiphase perfusion maps **c** with and **d** without flip angle sweep

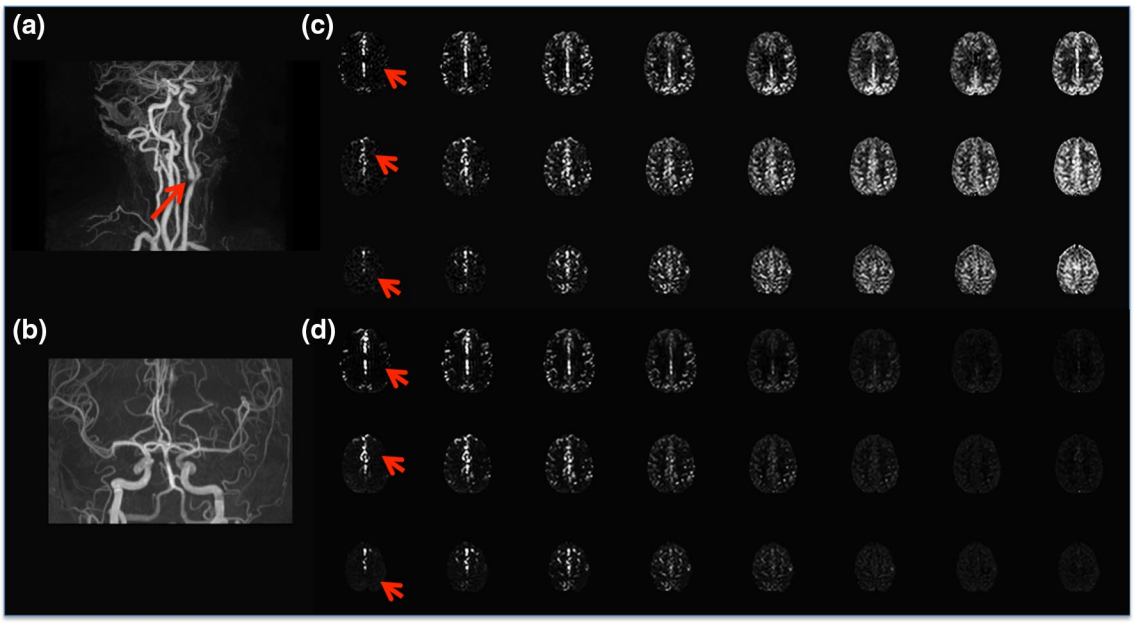

Fig. 7 Data from a patient with severe stenosis in the left ICA. **a** Carotid and **b** intracranial angiography. Multiphase perfusion maps **c** with and **d** without flip angle sweep

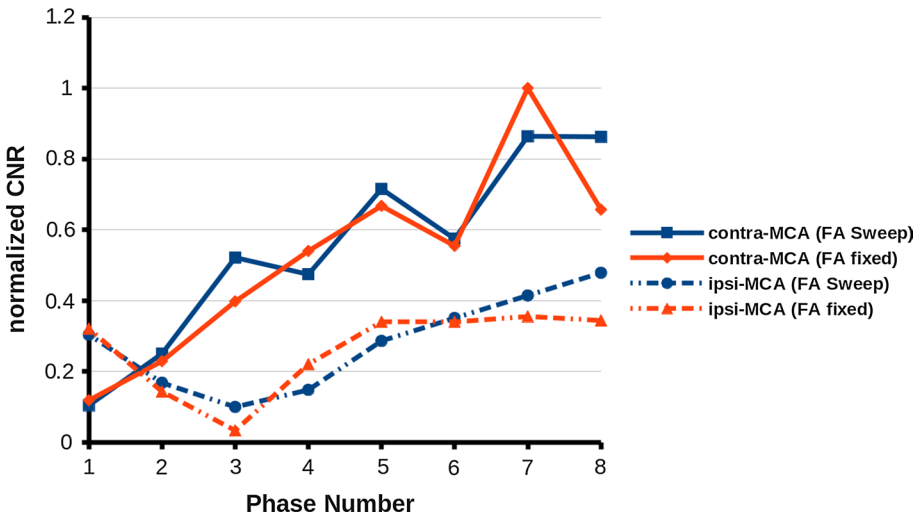

Fig. 8 CNR evolution over the phases for the FA sweep method and conventional method for the patient whose maps are shown in Fig. 7. CNR values were calculated for the region irrigated by the middle cerebral artery (MCA), for both hemispheres, ipsi and contralateral to the stenosis

In more than half of the patients with delayed transit time, the neurologist found difficulties in giving an accurate diagnosis due to the loss of information for long PLDs when using the conventional multi-PLD ASL method. The FA sweep approach improved such assessment, whose reports had a higher agreement with the MRA reports. For the critical carotid stenosis example shown in Fig. 4, there is a delayed transit time on both hemispheres, as shown in Fig. 5a. However, a careful analysis of the perfusion maps obtained by FA sweep method enabled the conclusion that the right hemisphere (with a carotid occlusion) is irrigated by the arterial blood coming from the left hemisphere due to vascular regulatory mechanisms, as collateral flow. Such a conclusion was only possible when analyzing all the phases. The lower CNR of images acquired by the conventional multi-PLD ASL method hampered the assessment of perfusion maps for long PLDs and difficulted the correct diagnosis.

The ability of this method to show perfusion dynamics was confirmed by the neurologist, who could observe subtle differences in patients' perfusion between hemispheres, as shown in Figs. 6 and 7. By evaluating images acquired using the FA sweep method, the neurologist could detect a small difference visible until the sixth PLD, which was hardly seen with the maps obtained by the conventional method. In the critical carotid stenosis example shown in Fig. 9, the TOF

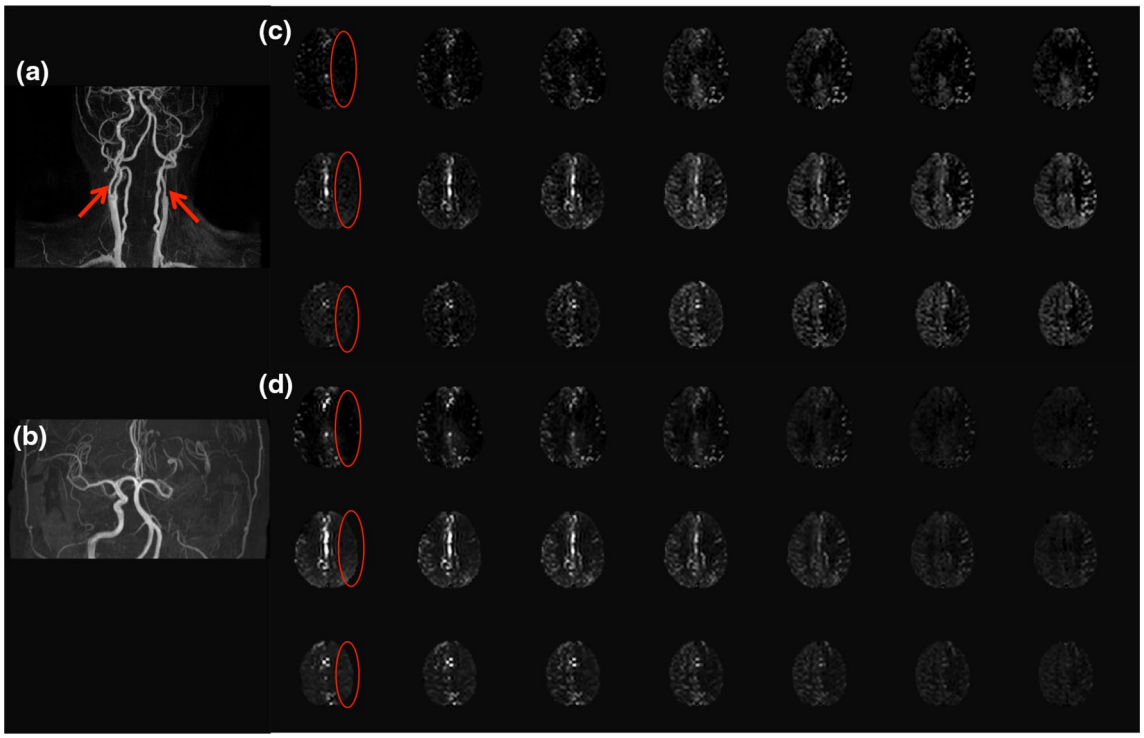

Fig. 9 Data from a patient with an obstruction in the left ICA and 70% stenosis in the right ICA. **a** Carotid and **b** intracranial angiography. Multiphase maps **c** with and **d** without flip angle sweep

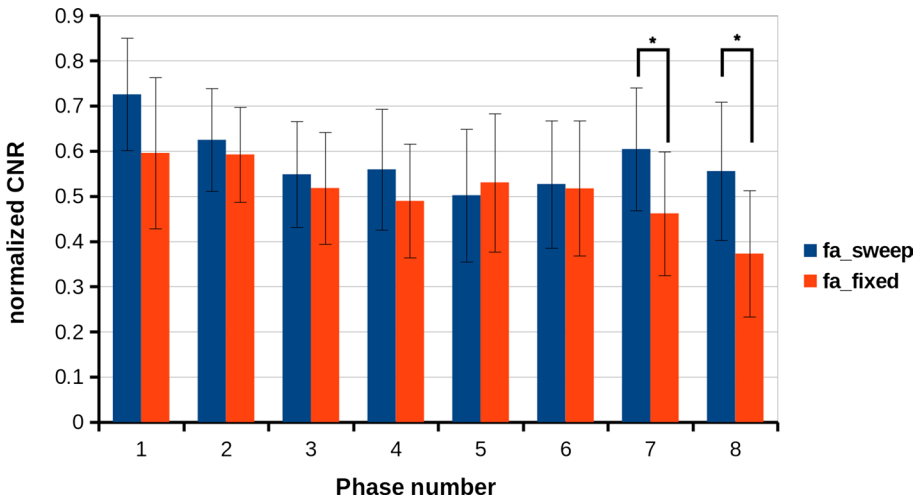

Fig. 10 Mean contrast-to-noise ratio for all 13 patients included in this study (mean ± standard deviation) for the FA sweep (blue) and FA fixed (red) methods (*p-FWE < 0.00625)

image shows a stenosis higher than 70% on the left side of the internal carotid artery (ICA), which results in prolonged transit time and delayed brain perfusion. The same pattern is observed by the analysis of ASL multi-PLD maps, which shows perfusion reduction in the left MCA in the first phases with prolonged ATT. Over the phases, both sides tend to be the same.

Although the patients were classified as asymptomatic for brain lesions, all of them showed alterations in cerebral hemodynamics, which may increase their risk for ischemic stroke [35, 36]. Most patients reported flow reduction in MCA vascular territory, which is directly irrigated by ICA. Moreover, delayed transit times were observed, even though the perfusion map for a long PLD was similar for both contralateral and ipsilateral hemispheres. Such results are consistent with the recent literature that reported hemispherical asymmetry of arterial transit time is related to severe ICA stenosis in ACAS patients, even though no

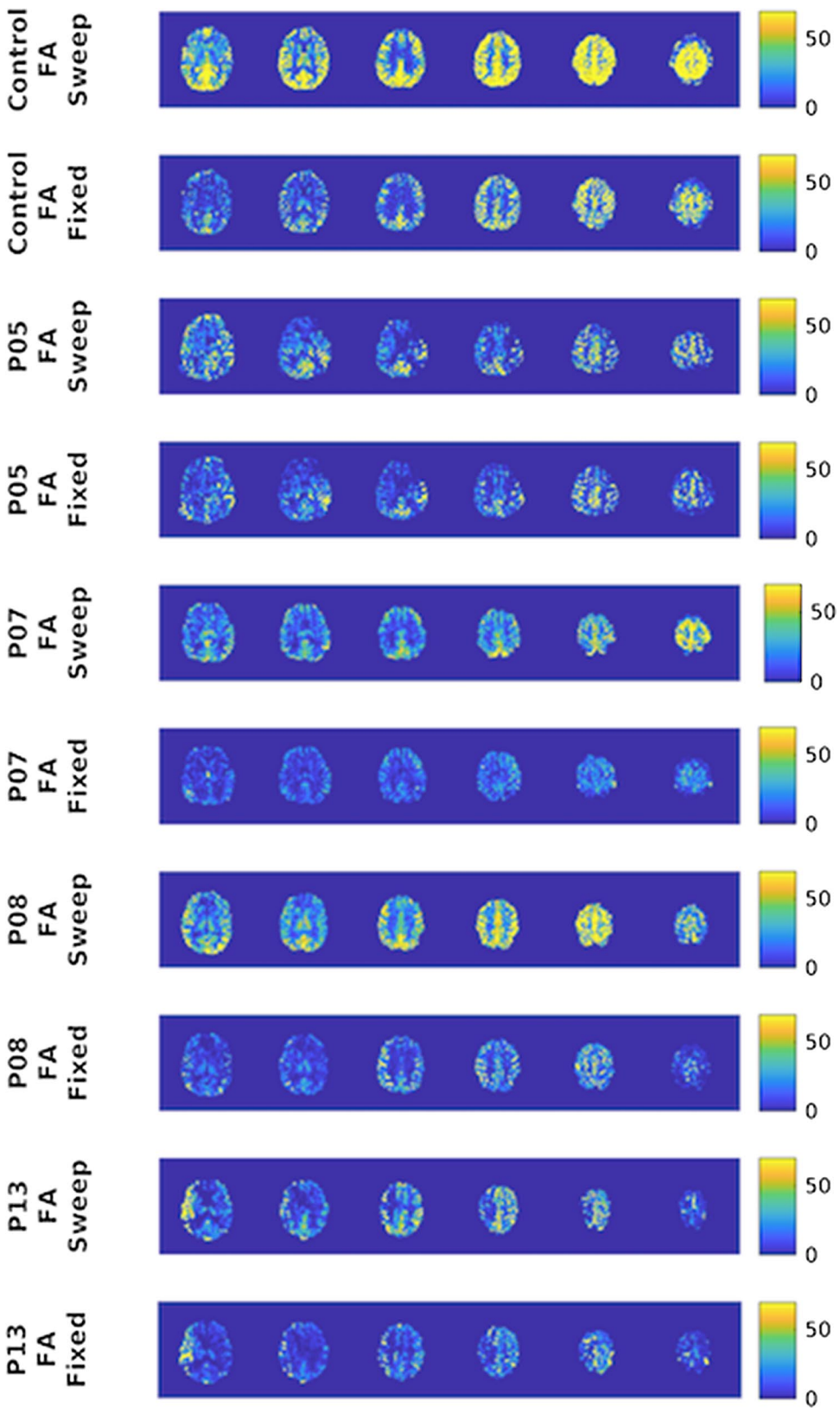

Fig. 11 Quantitative CBF maps for a representative healthy control and four examples of CAS patients for both multi-PLD ASL FA sweep and FA fixed methods. Scales unity are mL/100 g/min

CBF asymmetry was observed [37]. The observed alteration in cerebral hemodynamics of the patients may be related to impaired cognition usually observed in ACAS patients [38, 39]. Therefore, the dynamic investigation of cerebral perfusion is essential to characterize such patients.

Differently from the healthy subjects, the patients' mean CNR of all phases was higher for the FA sweep methods, although the difference was only significant for the last two PLDs. This difference for the first phases can be explained considering the higher sSNR for the FA sweep method as well as the delayed transit time for the patients. Since the blood did not fully arrive in the first PLDs, the mean signal intensity of GM and WM are comparable, equally lowering the CNR for both methods, which highlights the higher sSNR of the FA sweep method.

It is important to mention that even though we used the flip angle for the fixed FA approach within an acceptable range from the previous studies [15, 16], it was not specifically optimized in this study and might not be optimal.

The main benefit of the proposed modification in the Look–Locker readout for multi-PLD ASL is to improve the inspection of latter PLDs for patients with delayed transit time, helping the observation of, e.g., collateral flow (P05—Fig. 4). However, it is also possible to run the analysis under the kinetic model for ASL signal [19, 22] to perform the CBF quantification, taking advantage of higher SNR of the FA sweep approach when compared to the FA fixed.

In conclusion, we successfully assessed brain perfusion of patients with ICA stenosis using the multi-PLD ASL with flip angle sweep. The methodology was able to show subtle individual differences, which may help future studies on the management of the asymptomatic cerebrovascular disease. Moreover, we observed prolonged arterial transit time in patients, although they were considered asymptomatic, suggesting that it is not an adequate term to characterize them.

Acknowledgements The authors would like to acknowledge Angela Cristina Pregnolato Giampedro for editing the manuscript for language and style. This work was supported by São Paulo Research Foundation (FAPESP) (Grant # 2013/23740-0), financed in part by the Coordenação de Aperfeiçoamento de Pessoal de Nível Superior—Brasil (CAPES)—Finance Code 001, and by the Conselho Nacional de Desenvolvimento Científico e Tecnológico (CNPq) (Grant # 140110/2016-0).

Author contributions AMP contributed to study conception and design, acquisition of data, analysis, and interpretation of data and drafting of the manuscript. RFL contributed to acquisition of data, analysis, and interpretation of data and critical revision. BUF contributed to study conception and design and acquisition of data. ACS contributed to the analysis and interpretation of data. OMPN contributed to the analysis and interpretation of data. FFP contributed to study conception and design, data acquisition, analysis and interpretation of data, and critical revision.

Compliance with ethical standards

Conflict of interest On behalf of all the authors, the corresponding author states that there is no conflict of interest.

Ethical approval Human in vivo data were acquired in accordance with the guidelines set by the ethics committee of the University os São Paulo and after obtaining written informed consent from the subjects.

References

1. Salinet AS, Haunton VJ, Panerai RB, Robinson TG (2013) A systematic review of cerebral hemodynamic responses to neural activation following stroke. J Neurol 260(11):2715–2721
2. Ostergaard L, Jespersen SN, Engedahl T, Gutierrez Jimenez E, Ashkanian M, Hansen MB, Eskildsen S, Mouridsen K (2015) Capillary dysfunction: its detection and causative role in dementias and stroke. Curr Neurol Neurosci Rep 15(6):37
3. de Weerd M, Greving JP, Hedblad B, Lorenz MW, Mathiesen EB, O'Leary DH, Rosvall M, Sitzer M, de Borst GJ, Buskens E, Bots ML (2014) Prediction of asymptomatic carotid artery stenosis in the general population: identification of high-risk groups. Stroke 45(8):2366–2371
4. Detre JA, Leigh JS, Williams DS, Koretsky AP (1992) Perfusion imaging. Magnet Reson Med 23(1):37–45
5. Williams DS, Detre JA, Leigh JS, Koretsky AP (1992) Magnetic resonance imaging of perfusion using spin inversion of arterial water. Proc Natl Acad Sci USA 89(1):212–216
6. Lan L, Leng X, Abrigo J, Fang H, Ip VH, Soo YO, Leung TW, Yu SC, WONG LK (2016) Diminished signal intensities distal to intracranial arterial stenosis on time-of-flight MR angiography might indicate delayed cerebral perfusion. Cerebrovasc Dis 42(3–4):232–239
7. Grubb RL Jr, Derdeyn CP, Videen TO, Carpenter DA, Powers WJ (2016) Relative mean transit time predicts subsequent stroke in symptomatic carotid occlusion. J Stroke Cerebrovasc Dis 25(6):1421–1424
8. Tsujikawa T, Kimura H, Matsuda T, Fujiwara Y, Isozaki M, Kikuta K, Okazawa H (2016) Arterial transit time mapping obtained by pulsed continuous 3D ASL imaging with multiple post-label delay acquisitions: comparative study with PET-CBF in patients with chronic occlusive cerebrovascular disease. PLoS ONE 11(6):e0156005
9. Johnston ME, Lu K, Maldjian JA, Jung Y (2015) Multi-TI arterial spin labeling MRI with variable TR and bolus duration for cerebral blood flow and arterial transit time mapping. IEEE Trans Med Imaging 34(6):1392–1402
10. Lou X, Yu S, Scalzo F, Starkman S, Ali LK, Kim D, Rao NM, Hinman JD, Vespa PM, Jahan R, Tateshima S, Gonzalez NR, Duckwiler GR, Saver JL, Yoo B, Salamon N, Lyu J, Ma L, Wang DJ, Liebeskind DS (2017) Multi-delay ASL can identify leptomeningeal collateral perfusion in endovascular therapy of ischemic stroke. Oncotarget 8(2):2437–2443
11. Schmid S, Teeuwisse WM, Lu H, van Osch MJ (2015) Time-efficient determination of spin compartments by time-encoded pCASL T2-relaxation-under-spin-tagging and its application in hemodynamic characterization of the cerebral border zones. Neuroimage 123:72–79
12. Zhang X, Ingo C, Teeuwisse WM, Chen Z, van Osch MJP (2018) Comparison of perfusion signal acquired by arterial spin labeling-prepared intravoxel incoherent motion (IVIM) MRI and conventional IVIM MRI to unravel the origin of the IVIM signal. Magn Reson Med 79(2):723–729

13. Lawrence KS, Owen D, Wang DJJ (2012) A two-stage approach for measuring vascular water exchange and arterial transit time by diffusion-weighted perfusion MRI. Magnet Reson Med 67(5):1275–1284
14. Hales PW, Clark CA (2013) Combined arterial spin labeling and diffusion-weighted imaging for noninvasive estimation of capillary volume fraction and permeability-surface product in the human brain. J Cerebr Blood F Met 33(1):67–75
15. Gunther M, Bock M, Schad LR (2001) Arterial spin labeling in combination with a look-locker sampling strategy: inflow turbo-sampling EPI-FAIR (ITS-FAIR). Magn Reson Med 46(5):974–984
16. Varela M, Petersen ET, Golay X, Hajnal JV (2015) Cerebral blood flow measurements in infants using look-locker arterial spin labeling. J Magn Reson Imaging 41(6):1591–1600
17. Francis ST, Bowtell R, Gowland PA (2008) Modeling and optimization of Look-Locker spin labeling for measuring perfusion and transit time changes in activation studies taking into account arterial blood volume. Magn Reson Med 59(2):316–325
18. van der Plas MCE, Teeuwisse WM, Schmid S, Chappell M, van Osch MJP (2019) High temporal resolution arterial spin labeling MRI with whole-brain coverage by combining time-encoding with Look-Locker and simultaneous multi-slice imaging. Magn Reson Med 81(6):3734–3744
19. Golay X, Petersen ET, Hui F (2005) Pulsed star labeling of arterial regions (PULSAR): a robust regional perfusion technique for high field imaging. Magn Reson Med 53(1):15–21
20. von Samson-Himmelstjerna F, Madai VI, Sobesky J, Guenther M (2016) Walsh-ordered hadamard time-encoded pseudocontinuous ASL (WH pCASL). Magn Reson Med 76(6):1814–1824
21. Wells JA, Lythgoe MF, Gadian DG, Ordidge RJ, Thomas DL (2010) In vivo Hadamard encoded continuous arterial spin labeling (H-CASL). Magn Reson Med 63(4):1111–1118
22. Buxton RB, Frank LR, Wong EC, Siewert B, Warach S, Edelman RR (1998) A general kinetic model for quantitative perfusion imaging with arterial spin labeling. Magn Reson Med 40(3):383–396
23. Chappell MA, Groves AR, Whitcher B, Woolrich MW (2009) Variational bayesian inference for a nonlinear forward model. IEEE Trans Signal Process 57(1):223–236
24. Groves AR, Chappell MA, Woolrich MW (2009) Combined spatial and non-spatial prior for inference on MRI time-series. Neuroimage 45(3):795–809
25. Jenkinson M, Beckmann CF, Behrens TE, Woolrich MW, Smith SM (2012) Fsl. Neuroimage 62(2):782–790
26. Pfefferbaum A, Chanraud S, Pitel AL, Shankaranarayanan A, Alsop DC, Rohlfing T, Sullivan EV (2010) Volumetric cerebral perfusion imaging in healthy adults: regional distribution, laterality, and repeatability of pulsed continuous arterial spin labeling (PCASL). Psychiatry Res 182(3):266–273
27. Qin Q, Huang AJ, Hua J, Desmond JE, Stevens RD, van Zijl PC (2014) Three-dimensional whole-brain perfusion quantification using pseudo-continuous arterial spin labeling MRI at multiple post-labeling delays: accounting for both arterial transit time and impulse response function. NMR Biomed 27(2):116–128
28. Chen Y, Wang DJ, Detre JA (2012) Comparison of arterial transit times estimated using arterial spin labeling. MAGMA 25(2):135–144
29. Hara S, Tanaka Y, Ueda Y, Hayashi S, Inaji M, Ishiwata K, Ishii K, Maehara T, Nariai T (2017) Noninvasive evaluation of CBF and perfusion delay of moyamoya disease using arterial spin-labeling MRI with Multiple postlabeling delays: comparison with. AJNR Am J Neuroradiol 38(4):696–702
30. Haga S, Morioka T, Shimogawa T, Akiyama T, Murao K, Kanazawa Y, Sayama T, Arakawa S (2016) Arterial spin labeling perfusion magnetic resonance image with dual postlabeling delay: a correlative study with acetazolamide loading (123)I-iodoamphetamine Single-Photon emission computed tomography. J Stroke Cerebrovasc Dis 25(1):1–6
31. Paschoal AM, Leoni RF, Santos AC, Foerster BU, Paiva FF (2015) ASL contrast optimization in multiphase STAR labeling using variable flip angle. In: 21st annual meeting of the organization for human brain mapping, Honolulu, p 1857
32. Paschoal AM, Leoni RF, Santos AC, Foerster BU, Paiva FF (2017) Improving arterial spin labeling acquisition to reduce the effect of delayed arrival time. In: ISMRM 25th annual meeting & exhibition, Honolulu, p 1496
33. MacIntosh BJ, Filippini N, Chappell MA, Woolrich MW, Mackay CE, Jezzard P (2010) Assessment of arterial arrival times derived from multiple inversion time pulsed arterial spin labeling MRI. Magn Reson Med 63(3):641–647
34. MacIntosh BJ, Lindsay AC, Kylintireas I, Kuker W, Günther M, Robson MD, Kennedy J, Choudhury RP, Jezzard P (2010) Multiple inflow pulsed arterial spin-labeling reveals delays in the arterial arrival time in minor stroke and transient ischemic attack. AJNR Am J Neuroradiol 31(10):1892–1894
35. Wang T, Xiao F, Wu G, Fang J, Sun Z, Feng H, Zhang J, Xu H (2017) Impairments in brain perfusion, metabolites, functional connectivity, and cognition in severe asymptomatic carotid stenosis patients: an integrated MRI study. Neural Plast 2017:8738714
36. Camargo AP, Silva P, Rodrigues G, Camilo M, Paschoal A, Barreira C, Abud D, Leoni R, Pontes-Neto OM (2018) Cerebral perfusion, functional connectivity and cognitive profile of patients with assymptomatic carotid stenosis. Stroke 49:ATP422
37. Chen YF, Tang SC, Wu WC, Kao HL, Kuo YS, Yang SC (2017) Alterations of cerebral perfusion in asymptomatic internal carotid artery steno-occlusive disease. Sci Rep 7(1):1841
38. Xiang J, Zhang T, Yang QW, Liu J, Chen Y, Cui M, Yin ZG, Li L, Wang YJ, Li J, Zhou HD (2013) Carotid artery atherosclerosis is correlated with cognitive impairment in an elderly urban Chinese non-stroke population. J Clin Neurosci 20(11):1571–1575
39. Wang T, Mei B, Zhang J (2016) Atherosclerotic carotid stenosis and cognitive function. Clin Neurol Neurosurg 146:64–70